



Metformin enhances mitochondrial biogenesis and thermogenesis in brown adipocytes of mice

Iara Karise^a, Thereza Cristina Bargut^a, Mariano del Sol^b, Marcia Barbosa Aguila^a, Carlos A. Mandarim-de-Lacerda^{a,*,1}

^a Laboratory of Morphometry, Metabolism and Cardiovascular Disease, Biomedical Center, Institute of Biology, The University of the State of Rio de Janeiro, Rio de Janeiro, Brazil

^b Doctoral Program in Morphological Sciences, Universidad de La Frontera, Temuco, Chile



ARTICLE INFO

Keywords:
Brown adipose tissue
Thermogenesis
Metformin
Fructose
Mouse

ABSTRACT

Aims: We studied the effect of metformin on the brown adipose tissue (BAT) in a fructose-rich-fed model, focusing on BAT proliferation, differentiation, and thermogenic markers.

Main methods: C57Bl/6 mice received isoenergetic diets for ten weeks: control (C) or high-fructose (F). For additional eight weeks, animals received metformin hydrochloride (M, 250 mg/kg/day) or saline. After sacrifice, BAT and white fat pads were prepared for light microscopy and molecular analyses.

Key findings: Body mass gain, white fat pads, and adiposity index were not different among the groups. There was a reduction in energy intake in the F group and energy expenditure in the F and FM groups. Metformin led to a more massive BAT in both groups CM and FM, associated with a higher adipocyte proliferation (β 1-adrenergic receptor, proliferating cell nuclear antigen, and vascular endothelial growth factor), and differentiation (PR domain containing 16, bone morphogenetic protein 7), in part by activating 5' adenosine monophosphate-activated protein kinase. Metformin also enhanced thermogenic markers in the BAT (uncoupling protein type 1, peroxisome proliferator-activated receptor gamma coactivator-1 alpha) through adrenergic stimuli and fibroblast growth factor 21. Metformin might improve mitochondrial biogenesis in the BAT (nuclear respiratory factor 1, mitochondrial transcription factor A), lipolysis (perilipin, adipose triglyceride lipase, hormone-sensitive lipase), and fatty acid uptake (lipoprotein lipase, cluster of differentiation 36, adipocyte protein 2).

Significance: Metformin effects are not linked to body mass changes, but affect BAT thermogenesis, mitochondrial biogenesis, and fatty acid uptake. Therefore, BAT may be a metformin adjuvant target for the treatment of metabolic disorders.

1. Introduction

The brown adipose tissue (BAT) dissipates energy in heat form, promoting thermogenesis through the presence of uncoupling protein (UCP) 1 [1]. Studies demonstrated that BAT could be activated in adult

humans [2–4], as seen in cases of loss of body mass (BM) [5]. Also, cold-exposure might enhance BAT activity [6,7]. Brown adipocytes can proliferate and start brown adipogenesis when BAT is recruited, in a process under adrenergic control involving two key mediators: peroxisome proliferator-activated receptor gamma coactivator (PGC) 1-

Abbreviations: AMPK, adenosine monophosphate-activated protein kinase; AP2, adipocyte protein 2; BAT, brown adipose tissue; BM, body mass; β 1AR, beta-1 adrenergic receptor; β 3AR, beta-3 adrenergic receptor; BMP, bone morphogenetic protein; CD36, cluster of differentiation 36; cDNA, complementary DNA; CPT, carnitine palmitoyltransferase; FGF21, fibroblast growth factor 21; HSL, hormone sensitive lipase; LPL, lipoprotein lipase; mRNA, messenger RNA; NRF1, nuclear respiratory factor 1; pAMPK, human phosphorylated adenosine monophosphate activated protein kinase; PCNA, proliferating cell nuclear antigen; PGC1, peroxisome proliferator-activated receptor gamma coactivator 1; pHSL^{ser660}, phosphorylated hormone sensitive lipase on serine 660; PLIN1, perilipin; ATGL, adipose triglyceride lipase; PRDM, PR domain containing; SIRT, sirtuin; TFAM, mitochondrial transcription factor A; UCP, uncoupling protein; VEGF, vascular endothelial growth factor; WAT, white adipose tissue

* Corresponding author at: Laboratório de Morfometria, Metabolismo e Doença Cardiovascular, Centro Biomédico, Instituto de Biologia, Universidade do Estado do Rio de Janeiro, Av 28 de setembro 87 fds, Rio de Janeiro, RJ, 20551-030, Brazil.

E-mail addresses: iarakarise@hotmail.com (I. Karise), therezabargut@gmail.com (T.C. Bargut), mariano.delsol@ufrontera.cl (M. del Sol), mbaguila@uerj.br (M.B. Aguila), mandarim@uerj.br, mandarim.ca@gmail.com (C.A. Mandarim-de-Lacerda).

¹ Website: [Http://www.lmmc.uerj.br](http://www.lmmc.uerj.br)

<https://doi.org/10.1016/j.biopha.2019.01.021>

Received 12 October 2018; Received in revised form 4 January 2019; Accepted 6 January 2019

0753-3322/© 2019 Elsevier Masson SAS. This is an open access article under the CC BY-NC-ND license (<http://creativecommons.org/licenses/BY-NC-ND/4.0/>).

alpha, and PR domain containing (PRDM) 16. Differentiated brown adipocytes augment the expression of genes linked to lipid metabolism and mitochondrial function and ultimately of UCP1 [1,8]. Thus, different factors can induce and activate BAT, including cold [9], beta-adrenergic agonists [4], and drugs and nutritional compounds [8,10].

Fructose is becoming more and more a part of modern food in the Western world, being used in processed foods and sweetened soft drinks. Fructose is associated with insulin resistance, dyslipidemia and other metabolic diseases [11], and might promote white adipocyte hypertrophy, with local insulin resistance and inflammation [12,13], and dysregulated lipolysis [14]. Although the high fructose consumption in an isoenergetic diet does not cause obesity [15], the carbohydrate and lipid metabolisms are profoundly altered, influencing the liver and adipose tissue function [12,13,15].

Metformin, from the biguanides family, is a first-line drug in the treatment of diabetic patients [16] but has also been used to tackle inflammatory conditions [17], and some types of cancer [18]. Metformin had increased VLDL-triglycerides clearance in BAT, consequently lowering plasma triglycerides in mice [19], and led to BAT differentiation in diet-induced obese mice [20].

Significant uptake of metformin has been reported in the interscapular BAT depot of mouse [21]. However, the metformin effects on BAT, especially considering the association with a high-fructose diet are not known. Therefore, the current study aimed to investigate the possible action of metformin on BAT proliferation, differentiation, and thermogenic markers in a model with altered metabolism due to a high-fructose diet.

2. Material and methods

2.1. Ethical approval

The State University of Rio de Janeiro Ethics Committee for the Care and Use of Experimental Animals approved the study (protocol number CEUA/ 022/2015). The protocol followed the recommendations of the Guide for the Care and Use of Laboratory Animals of the National Institutes of Health (NIH Publication number 85-23, revised in 1996) and ARRIVE guidelines [22]. The animals were maintained in ventilated cages under controlled conditions (NexGen system, Allentown Inc., PA, USA, $20 \pm 2^\circ\text{C}$ and 12 h/12 h dark/light cycle), with free access to food and water. The terminology of genes and proteins were standardized [23]: gene symbols are italicized, with the first letter in uppercase; protein symbols are the same as the gene symbol but are not italicized, and all are uppercase.

2.2. Animals and diet

Three-months old nonconsanguineous male mice (C57BL/6) averaged with 24 ± 3 g were randomly divided into two groups ($n = 20$ /group, totaling 40 mice): control diet (C) or fructose diet (F, 47% of fructose), during ten weeks. The diets were isoenergetic (manufactured by PragSolucões, Jau, SP, Brazil) according to the recommendations of the American Institute of Nutrition for rodents (AIN93 M) [24] (Table 1). The high-fructose diet contained 47.37 g of fructose per 100 g of food, representing 50% of the total energy content of the food, already used by us [12,13,15] and others [25] to induce metabolic alterations.

After ten weeks, two new groups, including metformin hydrochloride (Pharmanostra, GO, Brazil), or vehicle (saline), were separated from each original group and studied for an additional eight weeks. Metformin was diluted in saline and orally given (250 mg/kg/day [26]) through orogastric gavage. The groups were formed ($n = 10$ /group) as described: C group (control diet for ten weeks, and control diet plus vehicle for eight additional weeks); CM group (control diet for ten weeks, and control diet plus metformin for eight additional weeks); F group (fructose diet for ten weeks, and fructose diet plus vehicle for

Table 1
Composition and energy content of the diets (control, C, and fructose, F).

Content (g)	Diets	
	C	F
Casein	140	140
Corn starch	620.7	146.4
Sucrose	100	100
Fructose	–	474.3
Soybean oil	40	40
Fibers	50	50
Vitamin mix ^a	10	10
Mineral mix ^a	35	35
Cystine	1.8	1.8
Choline	2.5	2.5
Antioxidant	0.008	0.008
Total	1000	1000
Energy (kJ)	15916	15916
Carbohydrates (% energy)	76	76
Proteins (% energy)	14	14
Lipids (% energy)	10	10

^a Mineral and vitamin mixtures follows the formulation of the American Institute of Nutrition (AIN93 M).

eight additional weeks); FM group (fructose diet for ten weeks, and fructose diet plus metformin for eight additional weeks).

The food intake was daily measured (the difference between the food supplied and the amount of food left in the cage), and energy intake was estimated (the product of food intake and the energy content of the diet).

2.3. Body mass, respiratory exchange ratio, and adiposity index

BM was measured weekly, and BM gain was determined as the BM difference between the 10th-week (the moment the groups were established) and the last week. The ratio between the sum of the fat masses divided by the BM was defined as the adiposity index.

The energy expenditure and respiratory exchange ratio (CO₂ production / O₂ uptake) were evaluated at the end of the experiment through indirect calorimetry (Apparatus Oxylet system, Panlab/Harvard, Barcelona, Spain). The monitoring system assessed respiratory metabolism by measuring the oxygen consumption (VO₂) and carbon dioxide production (VCO₂). Data were collected during 72 h after an acclimation period of 24 h (excluded from the analysis) and be an average over the entire testing period [27].

2.4. Sacrifice

Fasting mice for 6 h were anesthetized (150 mg/kg sodium pentobarbital i.p.), and then the interscapular BAT and white fat pads were dissected and weighed: epididymal (in the lower part of the abdomen, connected to the epididymis), retroperitoneal (in the posterior abdominal wall near the kidneys), and inguinal (subcutaneous fat between the lower part of the rib cage and the mid-thigh). Samples of the BAT were rapidly frozen and stored at -80°C or were kept in freshly prepared fixative solution (4% formaldehyde w/v, 0.1 M phosphate buffer, pH 7.2) for microscopy together with samples of inguinal adipose tissue. After embedding in Paraplast plus (Sigma-Aldrich, St. Louis, USA) and sectioning at 5- μm of thickness, sections were stained with hematoxylin and eosin. The observations and digital photomicrographs were obtained in a Nikon microscope (model 80i, and DS-Ri1 digital camera, Nikon Instruments, Inc., New York, USA).

2.5. Gene expression (qPCR)

Total RNA of BAT was extracted using Trizol reagent (Invitrogen, CA, USA). Nanovue spectroscopy (GE Life Sciences) was used to

Table 2

Data at sacrifice time.

Data	C	CM	F	FM
Body mass gain (g)	6.43 ± 0.67	5.78 ± 0.76	6.28 ± 0.48	5.95 ± 0.78
Food intake (g/day)	2.83 ± 0.33	2.86 ± 0.66	2.66 ± 0.48	2.74 ± 0.37
Energy intake (kJ/day)	45.04 ± 5.25	45.52 ± 10.50	42.34 ± 7.64	43.61 ± 5.89
EE (kJ/day)	12.62 ± 0.24	12.90 ± 0.05	11.02 ± 0.28 [‡]	11.56 ± 0.58 [§]
RER	0.995 ± 0.038	1.053 ± 0.039	1.015 ± 0.015	1.07 ± 0.032
Epididymal FPM (g)	0.233 ± 0.006	0.235 ± 0.006	0.234 ± 0.004	0.231 ± 0.008
Inguinal FPM (g)	0.194 ± 0.013	0.193 ± 0.007	0.191 ± 0.013	0.195 ± 0.015
Adiposity index (%)	1.716 ± 0.039	1.764 ± 0.093	1.760 ± 0.092	1.741 ± 0.076

Legend: EE, Energy expenditure; FPM, fat pad mass; RER, Respiratory exchange ratio. **Groups:** Control (C), fructose (F), metformin (M). Values are the means ± SD, n = 10/group. Significant differences are indicated (P < 0.05, one-way ANOVA and post-hoc test of Holm Sidak): F vs. C, ‡; FM vs. CM, §.

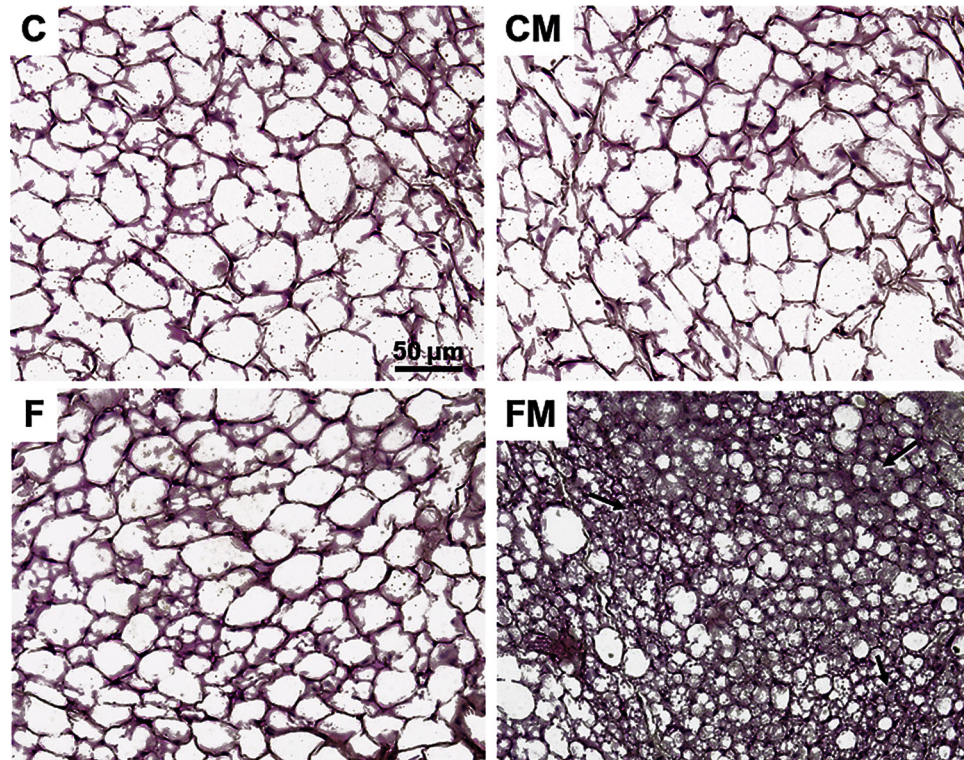


Fig. 1. Inguinal (subcutaneous) pad white adipocytes. **Groups:** C, control; CM, control plus metformin; F, fructose; FM, fructose plus metformin. Sections were stained with hematoxylin and eosin (same magnification to all photomicrographs). The overall unilocular appearance of white adipocytes was present in both C and CM groups. In the FM group, some adipocytes developed a 'brown-fat' presentation with multilocular adipocytes (arrows).

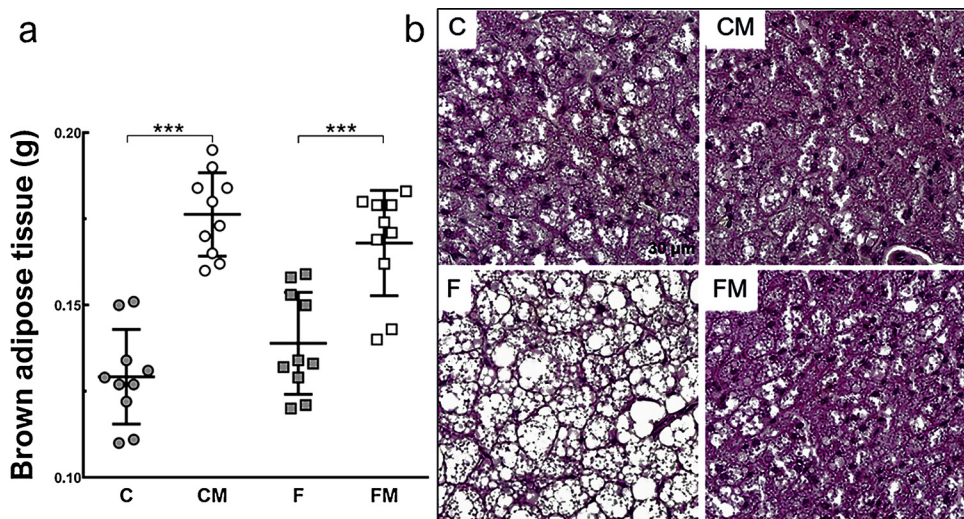


Fig. 2. Brown adipose tissue mass. **Groups:** C, control; CM, control plus metformin; F, fructose; FM, fructose plus metformin. Sections were stained with hematoxylin and eosin (same magnification to all photomicrographs). Mean ± SD (one-way ANOVA and posthoc test of Holm Sidak, ***P < 0.001). The overall multilocular appearance of brown adipocytes was present in both C and CM groups. In the F group, the adipocytes had more significant lipid droplets, a phenotype approaching 'white adipocytes' (arrows). The FM group showed brown adipocytes like the groups C and CM.

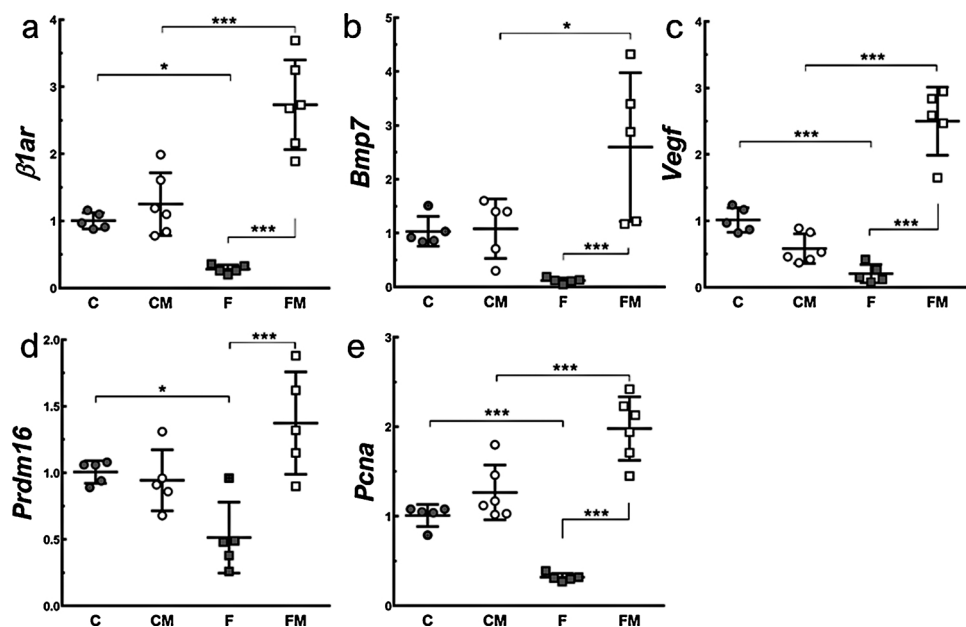


Fig. 3. Brown adipose tissue proliferation and differentiation markers. Groups: C, control; CM, control plus metformin; F, fructose; FM, fructose plus metformin (mean \pm SD, $n = 5$ –6/group, one-way ANOVA and posthoc test of Holm Sidak, $^*P < 0.05$, $^{***}P < 0.001$).

determine RNA amount. Then, RNA (1 μ g) was treated with DNase I (Invitrogen, CA, USA). Afterward, oligo (dT) primers for mRNA and superscript III reverse – transcriptase (both Invitrogen, CA, USA) were applied to the synthesis of first strand cDNA. The Biorad CFX96 cycler and the SYBR Green mix (Invitrogen, CA, USA) were used for qPCR (primers were detailed in supplemental Table S1). The endogenous β -actin was used to standardize the expression of the selected genes. After the pre-denaturation and polymerase-activation program (4 min at 95 °C), 44 cycles of 95 °C (10 s) and 60 °C (15 s) were tracked by a melting curve program (60–95 °C, a heating rate of 0.1 °C/s). Negative controls consisted of wells in which the cDNA was substituted for deionized water. The relative expression ratio of the mRNA was calculated using the equation $2^{-\Delta\Delta Ct}$, in which $-\Delta Ct$ represents the ratio between the number of cycles (CT) of the target genes with the endogenous control.

2.6. Protein level (Western blot)

The BAT total protein was extracted in homogenizing buffer containing protease inhibitors, and equivalent quantities of total protein were resuspended in SDS-containing sample buffer and heated for 5 min at 100 °C and separated by SDS-PAGE. After electrophoresis, the proteins were electroblotted onto polyvinyl difluoride transfer membranes (Amersham Biosciences, Piscataway, NJ, USA) – the blockade of the membrane used nonfat dry milk. The homogenates were incubated with the primary antibodies (Santa Cruz Biotechnology, CA, USA): AMPK alpha 1/2 (SC-25792) and pAMPKalpha 1/2^{thr172} (SC-33524); HSL (SC-25843) and UCP1 (33 kDa; SC-6529). Also, pHSL^{ser660} was used (orb335694; Biorbyt, Cambridge, UK). β -actin (SC81178; Santa Cruz Biotechnology, CA, USA) served as a loading control. Afterward, membranes were incubated with the corresponding secondary antibodies (anti-rabbit: SC2357; anti-goat: SC2354; and anti-mouse: SC2005; Santa Cruz Biotechnology, CA, USA). We used ECL for protein level detection system and the Molecular Imaging ChemiDoc XRS Systems (Bio-Rad, Hercules, CA, USA). The chemiluminescence intensity of the bands was quantified using the ImageJ software, version 1.51 (NIH, imagej.nih.gov/ij, USA). Endogenous control beta-actin was used to normalize the expression of the selected proteins. The absorbance values were measured.

2.7. Statistical analysis

The data were normally distributed (D'Agostino-Pearson "omnibus K2" test), and the variances of the groups were homogeneous (Browne-Forsythe test). Therefore, the values were shown as the mean, and the standard deviation (differences were analyzed with one-way analysis of variance, ANOVA, and the post hoc test of Holm – Sidak). The following comparisons were studied: CM vs. C; F vs. C; FM vs. CM; FM vs. F, and we reported the statistical differences (the P -value < 0.05 was considered significant, GraphPad Prism version 7.05 for Windows, GraphPad Software, La Jolla, CA, USA).

3. Results

3.1. Body mass gain, and food and energy intake

There was no difference in the BM gain among the groups. Food intake was not different before the treatment and after metformin administration (Table 2).

3.2. Energy expenditure and adiposity

The energy expenditure was lower in the F group compared to the C group (-13%, $P < 0.0001$), and in the FM group compared to the CM group (-10%, $P < 0.0001$). However, no differences were observed in the respiratory exchange ratio, epididymal fat pad, inguinal fat pad, and adiposity index (Table 2).

3.3. Inguinal (subcutaneous) WAT structure

White adipocytes were a unilocular cell containing a single huge droplet of lipid filling almost the entire cell in the inguinal fatty pad of the groups C, CM and F. Though, in the FM animals, clusters of brown-like adipocytes presenting smaller and multiple lipid droplets in the cytoplasm were observed (Fig. 1).

3.4. Metformin increased BAT mass

BAT was more massive in the CM group (+36%) than the C group, and the FM group (+21%) than the F group (Fig. 2A). The brown

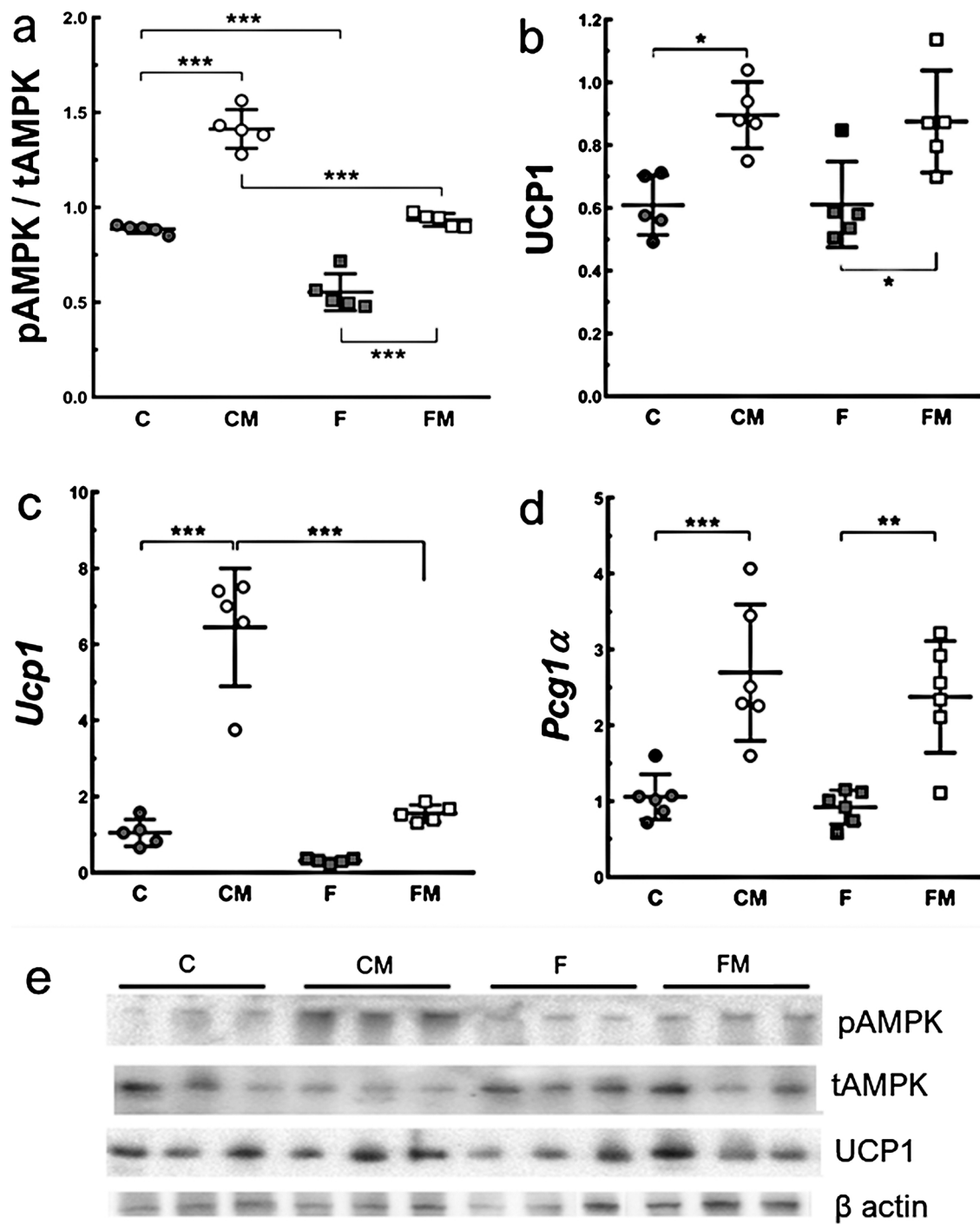


Fig. 4. Brown adipose tissue thermogenic markers. **Groups:** C, control; CM, control plus metformin; F, fructose; FM, fructose plus metformin (mean \pm SD, n = 5–6/group, one-way ANOVA and posthoc test of Holm Sidak, *P < 0.05, **P < 0.01, ***P < 0.001).

adipocytes in the groups C and CM were multilocular cells, but in the F group there was a fat infiltrates and more significant lipid droplets in the adipocytes, corresponding to the ‘white adipocyte-like’ phenotype. However, the multilocular structure of the brown adipocytes was restored in the FM group (Fig. 2B).

3.5. Metformin increased proliferation and differentiation markers in the BAT

The $\beta 1ar$ expression decreased in the F group (-72%) compared to the C group and raised in the FM group (+118% than the CM group, +869% than the F group). Also, *Bmp7* increased in the FM group

compared to the CM group (+140%), and the F group (+2065%). *Vegf* diminished in the F group compared to C group (-79%) but augmented in the FM group compared to the CM group (+523%) and the F group (+1100%) (Fig. 3A-C). *Prdm16* was lower in the F group compared to the C group (-49%) but higher in the FM group compared to the F group (+167%). *Pcna* diminished in the F group compared to the C group (-68%) but increased in the FM group compared to the CM group (+56%), and the F group (+523%) (Fig. 3D-E).

3.6. Metformin increased thermogenic markers in the BAT

The pAMPK/tAMPK ratio diminished in the F group compared to

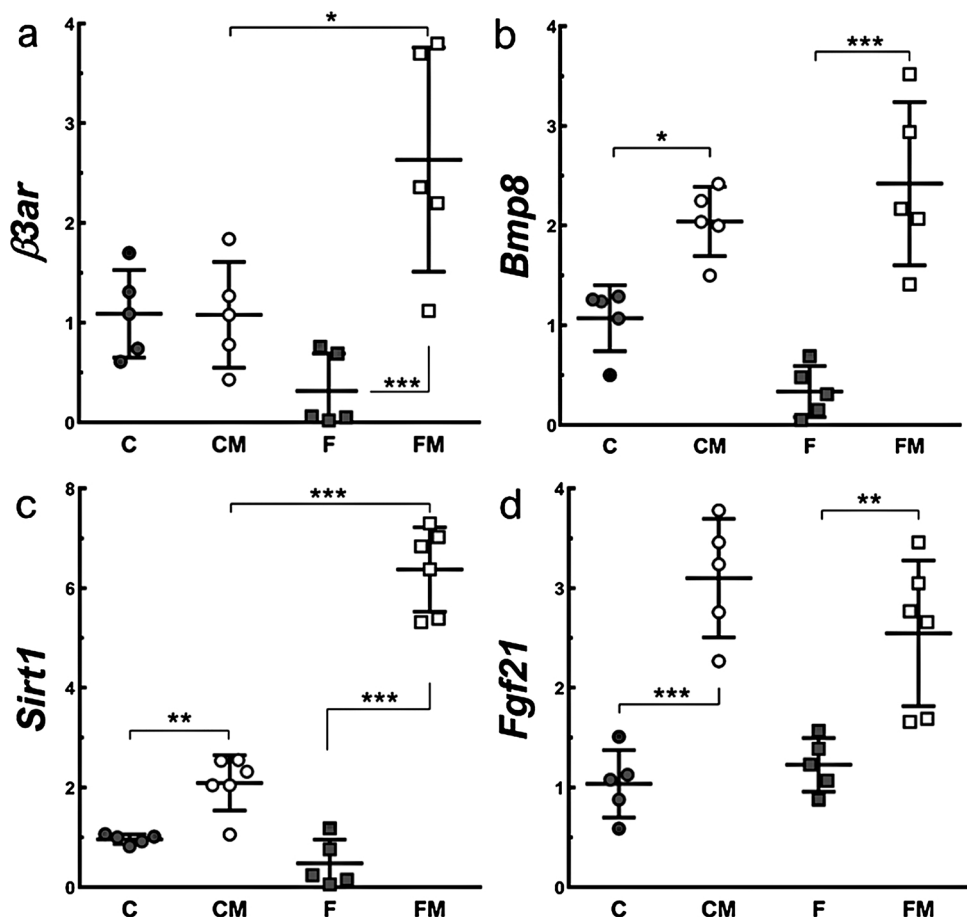


Fig. 5. Brown adipose tissue adrenergic-dependent and independent markers. **Groups:** C, control; CM, control plus metformin; F, fructose; FM, fructose plus metformin (mean \pm SD, n = 5–6/group, one-way ANOVA and posthoc test of Holm Sidak, *P < 0.05, **P < 0.01, ***P < 0.001).

the C group (-38%), and in the FM group compared to the CM group (-34%). However, pAMPK/tAMPK ratio was higher in the CM group than the C group (+60%), and in the FM group than the F group (+69%) (Fig. 4A).

Pgc1 alpha and *Ucp1* augmented in the CM group compared to the C group (+517% for both). *Pgc1 alpha* was also higher in the FM group than in the F group (+158%), while *UCP1* was lower in the FM group compared to the CM group (-76%). *UCP1* increased +47% in the CM group than the C group, and +43% in the FM group than the F group (Fig. 4B-D).

$\beta 3ar$ was higher in the FM group, +144% than the CM group, +734% than the F group. The CM group compared to C group showed augmented *Bmp8* (+90%), *Sirt1* (+117%), and *Fgf21* (+200%). The FM group compared to the F group showed increased *Bmp8* (+620%), *Sirt1* (+1226%) and *Fgf21* (+107%). *Sirt1* was also higher in the FM group than the CM group (+205%) (Fig. 5A-D).

3.7. Metformin enhanced mitochondrial biogenesis markers in the BAT

Nrf1 increased in the CM group compared to the C group (+212%), in the F group compared to the C group (+482%), and in the FM group compared to the CM group (+92%). *Tfam* was higher in the CM group than the C group (+136%) and in the FM group than the F group (+830%), but lower in the F group than the C group (-80%), and in the FM group compared to the CM group (-20%). *Cpt1* was elevated in the CM group compared to the C group (+254%) and in the F group than the C group (+145%) (Fig. 6A-C).

3.8. Metformin reduced substrate utilization markers in the BAT

Plin1 (*Perilipin*) was decreased in the F group than the C group (-68%) and in the FM group compared to the CM group (-63%). *Atgl* (+172%) and *Hsl* (+518%) were higher in the F group than the C group, and in the FM group compared to the CM group (*Atgl*, +72%; *Hsl*, +294%), but lower in the FM group than the F group (*Atgl*, -36%; *Hsl*, -48%) (Fig. 7A-C). The *phSL/tHSL* ratio was higher in the CM group than the C group (+47%) and in the F group than the C group (+81%) (Fig. 7D). Also, *Lpl* was higher in the F group than the C group (+200%), and in the FM group compared to the CM group (+118%). *Cd36* was elevated in the CM group compared to the C group (+80%), and in the F group than the C group (+64%), but it was lower in the FM group than the CM group (-23%). *Ap2* was higher in the F group compared to the C group (+117%), and in the FM group than the CM group (+107%), but it was lower in the FM group than the F group (-35%) (Fig. 8A-C).

4. Discussion

The study demonstrated that metformin has an action promoting the proliferation and differentiation of brown adipocytes and then an increase in BAT mass. Metformin also improves BAT thermogenic markers, mitochondrial biogenesis mediators, and markers of fatty acid utilization (metformin reduces *Atgl* and *Hsl*, which are known enzymes that hydrolyze triacylglycerol mobilizing the stored fats).

We chose to use a fructose model because data indicated that the high-fructose intake could alter the carbohydrate metabolism and liver both in mice and humans [28,29], and, therefore, we wanted to

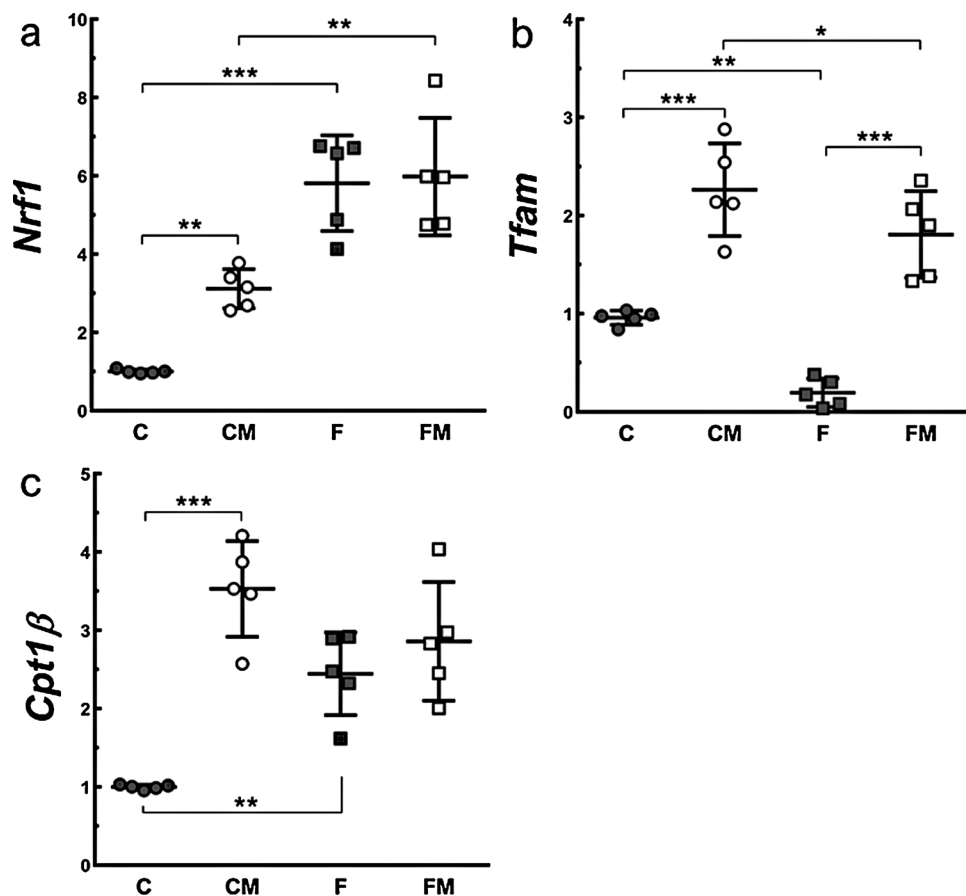


Fig. 6. Brown adipose tissue mitochondrial biogenesis markers. Groups: C, control; CM, control plus metformin; F, fructose; FM, fructose plus metformin (mean \pm SD, n = 5–6/group, one-way ANOVA and posthoc test of Holm Sidak, *P < 0.05, **P < 0.01, ***P < 0.001).

evaluate metformin effects under these adverse conditions. Importantly, the metabolic effects of the fructose intake were seen without a relevant BM gain, because the high-fructose diet was isoenergetic with the control diet and the food intake was not different among the groups. Consequently, the effects of metformin might be considered independent of alterations on BM [15,30]. Our previous studies with high-fructose consumption have demonstrated the induction of insulin resistance, increased plasma lipids and hepatic steatosis in this model, thus confirming that fructose can negatively affect metabolism in mice [15,31,32]. Herein, fructose reduced energy expenditure without effects on BM gain or fat pad masses.

Only recently BAT was perceived to be a metformin target [21]. Other studies have indicated that the lipid-lowering effect of metformin was due to increased VLDL-triglyceride clearance by BAT, which was accompanied by elevated lipolytic machinery and mitochondrial content [19]. The current study, to our knowledge, is the first attempting to associate BAT as a metformin target in a model of a high-fructose diet, and we have seen that metformin leads to an increase in *Pgc1-alpha* and UCP1. Thus, metformin enhanced BAT-related markers in WAT of mice fed a high-fat diet and increased *Ucp1* in 3T3-L1 adipocytes [33]. Metformin had also increased *Ucp1* in rat BAT [34], corroborating our results.

Metformin is recognized as a potent AMPK inducer [35] and on intracellular pathways that go beyond AMPK activation [36]. Metformin had increased AMPK activity in BAT of mouse leading to mitochondrial fatty acid transport and oxidation [19]. In cultured 3T3L1 adipocytes, metformin had reduced the endoplasmic reticulum stress in an AMPK-dependent manner [37] and, using compound C (an AMPK inhibitor), there was a reduction of IL-6 and TNF-alpha usually increased by metformin [38]. AMPK activation in BAT also enhanced

brown adipocyte formation in vitro [39]. Therefore, although the current study has a limitation because of the AMPK-dependent metformin effect was not measured directly by using an AMPK inhibitor, it is reasonable to hypothesize that the action of metformin on BAT uses the AMPK way, but it deserves further investigation.

Here, we observed an increase in the proliferation and differentiation markers leading to a greater BAT mass. Brown cell proliferation is mediated by β 1-AR [40] with the participation of PCNA [41] and VEGF [42]. Also, PRDM16 is a master regulator of adipocyte differentiation, and BMP7 is an essential inducer of this process [43], enhancing mitochondrial activity via increased fatty acid uptake and oxidation [44]. BAT hyperplasia may also occur in adipocytes under β 3-adrenergic stimuli [41]. Metformin had increased adrenergic signaling, especially in the FM group, including β 3-AR, BMP8, and SIRT1. BMP8B is involved in the thermogenic signaling and in expanding the BAT sympathetic tone [45], and SIRT1 may potentiate the response to β -adrenergic stimuli in the BAT [46].

Metformin had increased AMPK activity in WAT linked with the increased SIRT1 expression [47], which corroborates our results in the BAT. Furthermore, we suggest that metformin also increased FGF21 as another pathway of inducing BAT thermogenesis. Metformin is responsible for increasing FGF21 expression in white adipocytes [33] and in obese mice [20]. In BAT, FGF21 could elevate UCP1 expression [48].

Metformin effects elevating mitochondrial biogenesis markers in BAT were already reported [19]. NRF1 is the primary target of PGC1 alpha and regulates several genes involved in mitochondrial function and biogenesis, while TFAM is responsible for mitochondrial DNA replication and maintenance [49]. Also, the activation of the AMPK/PGC1 alpha-NRF axis was associated with the improvement of regulators of mitochondrial biogenesis [50], one of the possible

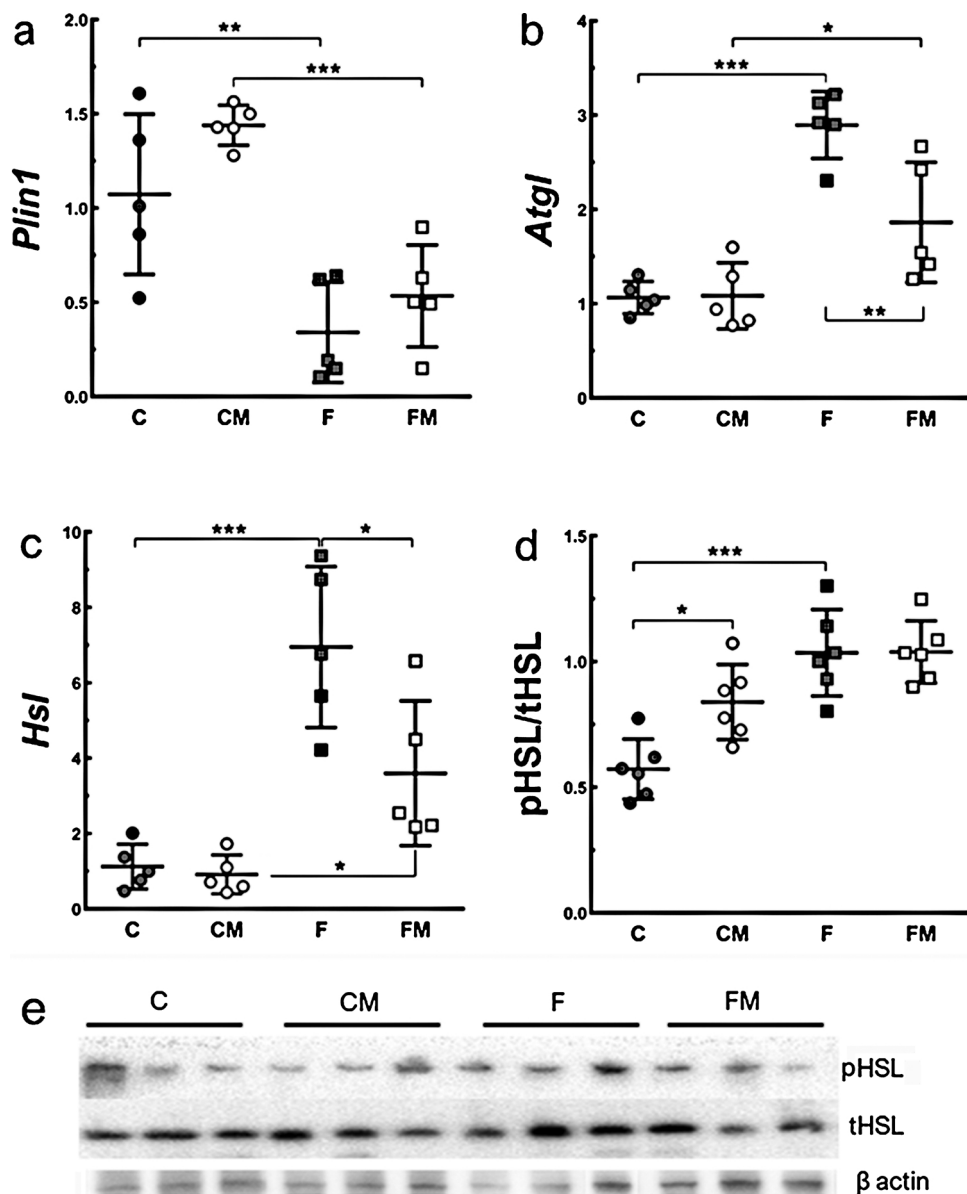


Fig. 7. Brown adipose tissue lipid uptake markers. **Groups:** C, control; CM, control plus metformin; F, fructose; FM, fructose plus metformin (mean \pm SD, n = 5–6/group, one-way ANOVA and posthoc test of Holm Sidak, *P < 0.05, **P < 0.01, ***P < 0.001).

mechanisms seen in the current study. Metformin enhanced CPT-1, an essential mitochondrial protein associated with fatty acid utilization and oxidation capacity. The inhibition of CPT-1 promotes impaired mitochondrial activity in brown adipocytes [44].

Thermogenesis uses fatty acids as a substrate, and the intracellular stocks should suffer lipolysis with the participation of perilipin, ATGL, and HSL [51]. The bloodstream is a source of fatty acids for usage or, more frequently, for replacement of the depots [52]. BAT activation also involves increased LPL and CD36, which are critical for fatty acid uptake [53]. We found an increased expression of CD36, indicating elevated fatty acid uptake. Since lipolytic genes continued to be higher in the FM group, we suggest that it contributed to reduced fat deposition in BAT in this group.

We housed mice at a temperature of 20 ± 2 °C, a condition in which mice have to increase metabolic heat production to maintain body temperature. This question is particularly important because of the translation to possible effects in humans [54]. A recent study confirmed that BAT has been already fully differentiated and therefore cannot be tested with cold, drugs, and nutrients in studies at around

21 °C. However, BAT expands and reduces the relative proportion of tissue lipids, and increases protein proportions, then forming more adipocytes [55]. These events are in agreement with our study, and thus reinforces that metformin can be considered a browning agent even in mice that were not at thermoneutrality.

Gene expression does not guarantee that the gene will be translated into a protein since gene and protein expressions do not always present similar results [56]. In mice, BAT is a small tissue, and adipose tissue has low protein content because of the high lipid content. We chose here to privilege the gene expression rather than the protein expression when it was not possible to perform both, and this is a limitation of the study.

5. Conclusion

The current study demonstrated that metformin stimulates BAT in mice metabolically stressed by a high-fructose diet, cellular proliferation (β 1AR, PCNA, and VEGF) and differentiation (PRDM16 and BMP7), possibly mediated by activating AMPK. Also, metformin

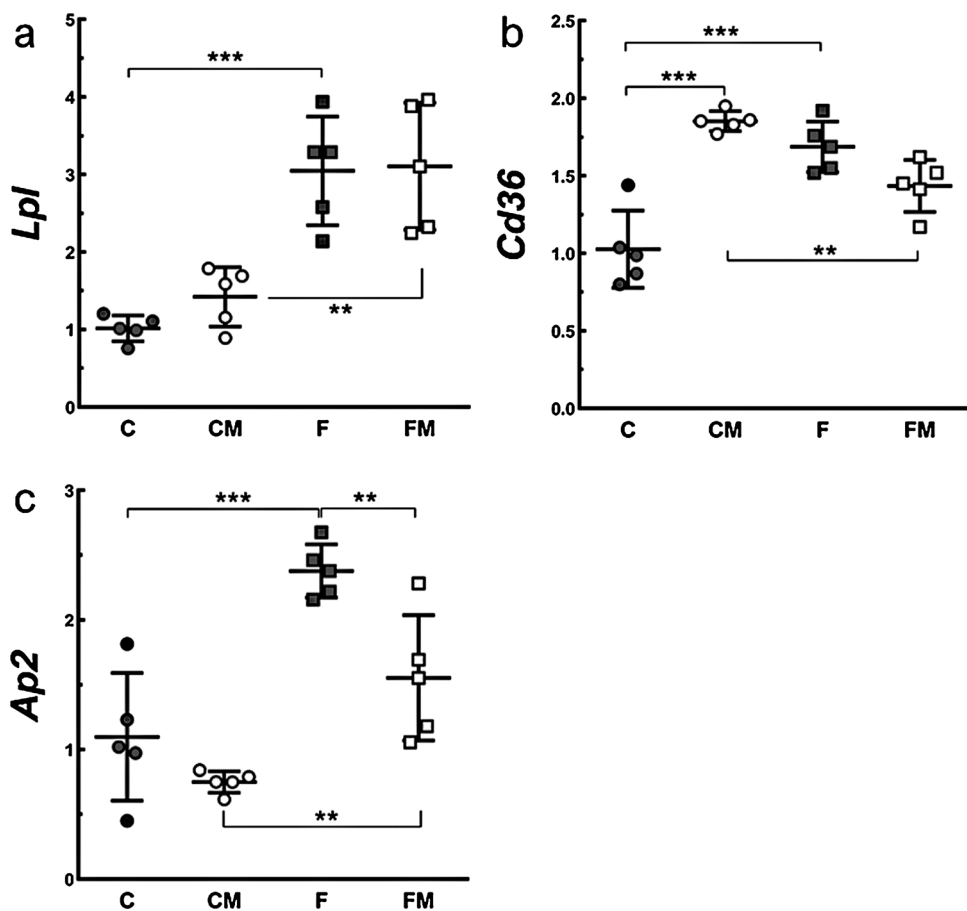


Fig. 8. Brown adipose tissue lipolysis markers. **Groups:** C, control; CM, control plus metformin; F, fructose; FM, fructose plus metformin (mean \pm SD, n = 5–6/group, one-way ANOVA and posthoc test of Holm Sidak, **P < 0.01, ***P < 0.001).

enhances thermogenic markers (UCP1 and PGC1alpha) and increases mediators of adrenergic stimuli and FGF21 expression, linked with enhanced mitochondrial biogenesis (NRF1 and TFAM) markers, and altered lipolysis (perilipin, ATGL, and HSL), and fatty acid uptake (LPL, CD36, and aP2) markers. Therefore, BAT may be an adjuvant metformin target for the treatment of a disorder of the metabolism, independent of alterations in BM.

Conflict of interest

None.

Acknowledgment

The study was supported by Conselho Nacional de Desenvolvimento Científico e Tecnológico (Brazil) (CNPq, Grant No 302.920/2016-1), Fundação Carlos Chagas Filho de Amparo à Pesquisa do Estado do Rio de Janeiro (Faperj, Grant No E-26/010.003.093 /2014, and E-26/202.935/2017), and Coordenação de Aperfeiçoamento de Pessoal de Nível Superior - Brazil (CAPES) - Finance Code 001. These foundations had no interference in the accomplishment and submission of the study.

Appendix A. Supplementary data

Supplementary material related to this article can be found, in the online version, at doi:<https://doi.org/10.1016/j.biopha.2019.01.021>.

References

[1] B. Cannon, J. Nedergaard, Brown adipose tissue: function and physiological

significance, *Physiol. Rev.* 84 (2004) 277–359, <https://doi.org/10.1152/physrev.00015.2003>.

- [2] J. Nedergaard, T. Bengtsson, B. Cannon, Unexpected evidence for active brown adipose tissue in adult humans, *Am. J. Physiol. Endocrinol. Metab.* 293 (2007), <https://doi.org/10.1152/ajpendo.00691.2006> E444–52.
- [3] A.M. Cypress, S. Lehman, G. Williams, I. Tal, D. Rodman, A.B. Goldfine, F.C. Kuo, E.L. Palmer, Y.H. Tseng, A. Doria, G.M. Kolodny, C.R. Kahn, Identification and importance of brown adipose tissue in adult humans, *N. Engl. J. Med.* 360 (2009) 1509–1517, <https://doi.org/10.1056/NEJMoa0810780>.
- [4] A.M. Cypress, L.S. Weiner, C. Roberts-Toler, E. Franquet Elia, S.H. Kessler, P.A. Kahn, J. English, K. Chatman, S.A. Trauger, A. Doria, G.M. Kolodny, Activation of human brown adipose tissue by a beta3-adrenergic receptor agonist, *Cell Metab.* 21 (2015) 33–38, <https://doi.org/10.1016/j.cmet.2014.12.009>.
- [5] G.H. Vrijen, N.D. Bouvy, G.J. Teule, B. Brans, J. Hoeks, P. Schrauwen, W.D. Van Marken Lichtenbelt, Increase in brown adipose tissue activity after weight loss in morbidly obese subjects, *J. Clin. Endocrinol. Metab.* 97 (2012), <https://doi.org/10.1210/jc.2012-1289> E1229–33.
- [6] T. Yoneshiro, S. Aita, M. Matsushita, T. Kayahara, T. Kameya, Y. Kawai, T. Iwanaga, M. Saito, Recruited brown adipose tissue as an antiobesity agent in humans, *J. Clin. Invest.* 123 (2013) 3404–3408, <https://doi.org/10.1172/JCI67803>.
- [7] M. Chondronikola, E. Volpi, E. Borsheim, C. Porter, P. Annamalai, S. Enerback, M.E. Lidell, M.K. Saraf, S.M. Labbe, N.M. Hurren, C. Yfanti, T. Chao, C.R. Andersen, F. Cesani, H. Hawkins, L.S. Sidossis, Brown adipose tissue improves whole-body glucose homeostasis and insulin sensitivity in humans, *Diabetes* 63 (2014) 4089–4099, <https://doi.org/10.2337/db14-0746>.
- [8] T.C. Bargut, M.B. Aguila, C.A. Mandarim-de-Lacerda, Brown adipose tissue: updates in cellular and molecular biology, *Tissue Cell* 48 (2016) 452–460, <https://doi.org/10.1016/j.tice.2016.08.001>.
- [9] A.M. Cypress, Y.-C. Chen, C. Sze, K. Wang, J. English, O. Chan, A.R. Holman, I. Tal, M.R. Palmer, G.M. Kolodny, Cold but not sympathomimetics activates human brown adipose tissue in vivo, *Proc. Natl. Acad. Sci.* 109 (2012) 10001–10005, <https://doi.org/10.1073/pnas.1207911109>.
- [10] M. Hibi, S. Oishi, M. Matsushita, T. Yoneshiro, T. Yamaguchi, C. Usui, K. Yasunaga, Y. Katsuragi, K. Kubota, S. Tanaka, M. Saito, Brown adipose tissue is involved in diet-induced thermogenesis and whole-body fat utilization in healthy humans, *Int. J. Obes. (Lond)* 40 (2016) 1655–1661, <https://doi.org/10.1038/ijo.2016.124>.
- [11] K.L. Stanhope, Sugar consumption, metabolic disease and obesity: the state of the controversy, *Crit. Rev. Clin. Lab. Sci.* 53 (2016) 52–67, <https://doi.org/10.3109/10408363.2015.1084990>.

[12] D.C. Magliano, A. Penna-de-Carvalho, M. Vazquez-Carrera, C.A. Mandarim-de-Lacerda, M.B. Aguila, Short-term administration of GW501516 improves inflammatory state in white adipose tissue and liver damage in high-fructose-fed mice through modulation of the renin-angiotensin system, *Endocrine* 50 (2015) 355–367, <https://doi.org/10.1007/s12020-015-0590-1>.

[13] T.C.L. Bargut, L.P. Santos, D.G.L. Machado, M.B. Aguila, C.A. Mandarim-de-Lacerda, Eicosapentaenoic acid (EPA) vs. Docosahexaenoic acid (DHA): effects in epididymal white adipose tissue of mice fed a high-fructose diet, *Prostaglandins Leukot. Essent. Fatty Acids* 123 (2017) 14–24, <https://doi.org/10.1016/j.plefa.2017.07.004>.

[14] B. Legeza, Z. Balazs, A. Odermatt, Fructose promotes the differentiation of 3T3-L1 adipocytes and accelerates lipid metabolism, *FEBS Lett.* 588 (2014) 490–496, <https://doi.org/10.1016/j.febslet.2013.12.014>.

[15] A. Schultz, D. Neil, M.B. Aguila, C.A. Mandarim-de-Lacerda, Hepatic adverse effects of fructose consumption independent of overweight/obesity, *Int. J. Mol. Sci.* 14 (2013) 21873–21886, <https://doi.org/10.3390/ijms141121873>.

[16] I. Thomas, B. Gregg, Metformin; a review of its history and future: from lilac to longevity, *Pediatr. Diabetes* 18 (2017) 10–16, <https://doi.org/10.1111/pedi.12473>.

[17] A. Pandey, S. Verma, V.L. Kumar, Metformin maintains mucosal integrity in an experimental model of colitis by inhibiting oxidative stress and pro-inflammatory signaling, *Biomed. Pharmacother.* 94 (2017) 1121–1128, <https://doi.org/10.1016/j.bioph.2017.08.020>.

[18] F.J. Fernandez-Fernandez, Antineoplastic potential of metformin in colorectal cancer, *Eur. J. Intern. Med.* 37 (2017) e22, <https://doi.org/10.1016/j.ejim.2016.08.034>.

[19] J.J. Geerling, M.R. Boon, G.C. van der Zon, S.A. van den Berg, A.M. van den Hoek, M. Lombers, H.M. Princen, L.M. Havekes, P.C. Rensen, B. Guigas, Metformin lowers plasma triglycerides by promoting VLDL-triglyceride clearance by brown adipose tissue in mice, *Diabetes* 63 (2014) 880–891, <https://doi.org/10.2337/db13-0194>.

[20] E.K. Kim, S.H. Lee, S.Y. Lee, J.K. Kim, J.Y. Jhun, H.S. Na, S.Y. Kim, J.Y. Choi, C.W. Yang, S.H. Park, M.L. Cho, Metformin ameliorates experimental-obesity-associated autoimmune arthritis by inducing FGF21 expression and brown adipocyte differentiation, *Exp. Mol. Med.* 50 (2018) e432, <https://doi.org/10.1038/emm.2017.245>.

[21] P. Breining, J.B. Jensen, E.I. Sundelin, L.C. Gormsen, S. Jakobsen, M. Busk, L. Rølighed, P. Bross, P. Fernandez-Guerra, L.K. Markussen, N.E. Rasmussen, J.B. Hansen, S.B. Pedersen, B. Richelsen, N. Jessen, Metformin targets brown adipose tissue in vivo and reduces oxygen consumption in vitro, *Diabetes Obes. Metab.* 20 (2018) 2264–2273, <https://doi.org/10.1111/dom.13362>.

[22] C. Kilkenny, W. Browne, I.C. Cuthill, M. Emerson, D.G. Altman, N.C.R.R.G.W. Group, Animal research: reporting in vivo experiments: the ARRIVE guidelines, *Br. J. Pharmacol.* 160 (2010) 1577–1579, <https://doi.org/10.1111/j.1476-5381.2010.00872.x>.

[23] M.T. Davison, Rules and guidelines for nomenclature of mouse genes. International Committee on Standardized Genetic Nomenclature for Mice, *Gene* 147 (1994) 157–160.

[24] P.G. Reeves, F.H. Nielsen, G.C. Fahey Jr, AIN-93 purified diets for laboratory rodents: final report of the American Institute of Nutrition ad hoc writing committee on the reformulation of the AIN-76A rodent diet, *J. Nutr.* 123 (1993) 1939–1951.

[25] N. Sharma, L. Li, C.M. Ecelbarger, Sex differences in renal and metabolic responses to a high-fructose diet in mice, *Am. J. Physiol. Renal Physiol.* 308 (2015) F400–F410, <https://doi.org/10.1152/ajprenal.00403.2014>.

[26] T. Ikeda, K. Iwata, H. Murakami, Inhibitory effect of metformin on intestinal glucose absorption in the perfused rat intestine, *Biochem. Pharmacol.* 59 (2000) 887–890.

[27] G. Livesey, M. Elia, Estimation of energy expenditure, net carbohydrate utilization, and net fat oxidation and synthesis by indirect calorimetry: evaluation of errors with special reference to the detailed composition of fuels, *Am. J. Clin. Nutr.* 47 (1988) 608–628.

[28] R. Kelishadi, M. Mansourian, M. Heidari-Beni, Association of fructose consumption and components of metabolic syndrome in human studies: a systematic review and meta-analysis, *Nutrition* 30 (2014) 503–510, <https://doi.org/10.1016/j.nut.2013.08.014>.

[29] C.L. Chou, C.H. Li, H. Lin, M.H. Liao, C.C. Wu, J.S. Chen, Y.M. Sue, T.C. Fang, Role of activating transcription factor 3 in fructose-induced metabolic syndrome in mice, *Hypertens. Res.* 41 (2018) 589–597, <https://doi.org/10.1038/s41440-018-0058-9>.

[30] S.K. Malin, S.R. Kashyap, Effects of metformin on weight loss: potential mechanisms, *Curr. Opin. Endocrinol. Diabet. Obes.* 21 (2014) 323–329, <https://doi.org/10.1097/MED.0000000000000095>.

[31] V.F. Motta, T.L. Bargut, M.B. Aguila, C.A. Mandarim-de-Lacerda, Treating fructose-induced metabolic changes in mice with high-intensity interval training: insights in the liver, white adipose tissue, and skeletal muscle, *J. Appl. Physiol.* 123 (2017) 1985 699–709, <https://doi.org/10.1152/japplphysiol.00154.2017>.

[32] A. Schultz, S. Barbosa-da-Silva, M.B. Aguila, C.A. Mandarim-de-Lacerda, Differences and similarities in hepatic lipogenesis, gluconeogenesis and oxidative imbalance in mice fed diets rich in fructose or sucrose, *Food Funct.* 6 (2015) 1684–1691, <https://doi.org/10.1039/c5fo00251f>.

[33] E.K. Kim, S.H. Lee, J.Y. Jhun, J.K. Byun, J.H. Jeong, S.Y. Lee, J.K. Kim, J.Y. Choi, M.L. Cho, Metformin prevents fatty liver and improves balance of White/Brown adipose in an obesity mouse model by inducing FGF21, *Mediators Inflamm.* 2016 (2016) 5813030, <https://doi.org/10.1155/2016/5813030>.

[34] I. Tokubuchi, Y. Tajiri, S. Iwata, K. Hara, N. Wada, T. Hashinaga, H. Nakayama, H. Mifune, K. Yamada, Beneficial effects of metformin on energy metabolism and visceral fat volume through a possible mechanism of fatty acid oxidation in human subjects and rats, *PLoS One* 12 (2017), <https://doi.org/10.1371/journal.pone.0171293> e0171293.

[35] G. Zhou, R. Myers, Y. Li, Y. Chen, X. Shen, J. Fenley-Melody, M. Wu, J. Ventre, T. Doeber, N. Fujii, N. Musi, M.F. Hirshman, L.J. Goodyear, D.E. Moller, Role of AMP-activated protein kinase in mechanism of metformin action, *J. Clin. Invest.* 108 (2001) 1167–1174, <https://doi.org/10.1172/JCI13505>.

[36] Y. Fujita, N. Inagaki, Metformin: new preparations and nonglycemic benefits, *Curr. Diab. Rep.* 17 (2017) 5, <https://doi.org/10.1007/s11892-017-0829-8>.

[37] A. Li, S. Zhang, J. Li, K. Liu, F. Huang, B. Liu, Metformin and resveratrol inhibit Drp1-mediated mitochondrial fission and prevent ER stress-associated NLRP3 inflammasome activation in the adipose tissue of diabetic mice, *Mol. Cell. Endocrinol.* 434 (2016) 36–47, <https://doi.org/10.1016/j.mce.2016.06.008>.

[38] Y. Jing, F. Wu, D. Li, L. Yang, Q. Li, R. Li, Metformin improves obesity-associated inflammation by altering macrophages polarization, *Mol. Cell. Endocrinol.* 461 (2018) 256–264, <https://doi.org/10.1016/j.mce.2017.09.025>.

[39] S. Wang, X. Liang, Q. Yang, X. Fu, M. Zhu, B.D. Rodgers, Q. Jiang, M.V. Dodson, M. Du, Resveratrol enhances brown adipocyte formation and function by activating AMP-activated protein kinase (AMPK) alpha1 in mice fed high-fat diet, *Mol. Nutr. Food Res.* 61 (2017), <https://doi.org/10.1002/mnfr.201600746>.

[40] G. Bronnikov, J. Houstek, J. Nedergaard, Beta-adrenergic, cAMP-mediated stimulation of proliferation of brown fat cells in primary culture. Mediation via beta 1 but not via beta 3 adrenoceptors, *J. Biol. Chem.* 267 (1992) 2006–2013.

[41] K. Fukano, Y. Okamatsu-Ogura, A. Tsubota, J. Nio-Kobayashi, K. Kimura, Cold exposure induces proliferation of mature brown adipocyte in a ss3-Adrenergic receptor-mediated pathway, *PLoS One* 11 (2016), <https://doi.org/10.1371/journal.pone.0166579> e0166579.

[42] I. Shimizu, T. Aprahamian, R. Kikuchi, A. Shimizu, K.N. Papanicolaou, S. MacLachlan, S. Maruyama, K. Walsh, Vascular rarefaction mediates whitening of brown fat in obesity, *J. Clin. Invest.* 124 (2014) 2099–2112, <https://doi.org/10.1172/JCI71643>.

[43] S. Kajimura, Promoting brown and beige adipocyte biogenesis through the PRDM16 pathway, *Int. J. Obes. Suppl.* 5 (2015) S11–S14, <https://doi.org/10.1038/ijosup.2015.4>.

[44] K.L. Townsend, D. An, M.D. Lynes, T.L. Huang, H. Zhang, L.J. Goodyear, Y.H. Tseng, Increased mitochondrial activity in BMP7-treated brown adipocytes, due to increased CPT1- and CD36-mediated fatty acid uptake, *Antioxid. Redox Signal.* 19 (2013) 243–257, <https://doi.org/10.1089/ars.2012.4536>.

[45] A.J. Whittle, S. Carobbio, L. Martins, M. Slawik, E. Hondares, M.J. Vazquez, D. Morgan, R.I. Csikasz, R. Gallego, S. Rodriguez-Cuenca, M. Dale, S. Virtue, F. Villarroya, B. Cannon, K. Rahmouni, M. Lopez, A. Vidal-Puig, BMP8B increases brown adipose tissue thermogenesis through both central and peripheral actions, *Cell* 149 (2012) 871–885, <https://doi.org/10.1016/j.cell.2012.02.066>.

[46] M. Boutant, M. Joffraud, S.S. Kulkarni, E. Garcia-Casarrubios, P.M. Garcia-Roves, J. Ratajczak, P.J. Fernandez-Marcos, A.M. Valverde, M. Serrano, C. Canto, SIRT1 enhances glucose tolerance by potentiating brown adipose tissue function, *Mol. Metab.* 4 (2015) 118–131, <https://doi.org/10.1016/j.molmet.2014.12.008>.

[47] P.W. Caton, J. Kieswich, M.M. Yaqoob, M.J. Holness, M.C. Sugden, Metformin opposes impaired AMPK and SIRT1 function and deleterious changes in core clock protein expression in white adipose tissue of genetically-obese db/db mice, *Diabetes Obes. Metab.* 13 (2011) 1097–1104, <https://doi.org/10.1111/j.1463-1326.2011.01466.x>.

[48] S. Keipert, M. Kutschke, D. Lamp, L. Brachthauser, F. Neff, C.W. Meyer, R. Oelkrug, A. Kharitonov, M. Jastroch, Genetic disruption of uncoupling protein 1 in mice renders brown adipose tissue a significant source of FGF21 secretion, *Mol. Metab.* 4 (2015) 537–542, <https://doi.org/10.1016/j.molmet.2015.04.006>.

[49] J.A. Williams, K. Zhao, S. Jin, W.X. Ding, New methods for monitoring mitochondrial biogenesis and mitophagy in vitro and in vivo, *Exp. Biol. Med. (Maywood)* 242 (2017) 781–787, <https://doi.org/10.1177/1535370216688802>.

[50] D. Kukidome, T. Nishikawa, K. Sonoda, K. Imoto, K. Fujisawa, M. Yano, H. Motoshima, T. Taguchi, T. Matsumura, E. Araki, Activation of AMP-activated protein kinase reduces hyperglycemia-induced mitochondrial reactive oxygen species production and promotes mitochondrial biogenesis in human umbilical vein endothelial cells, *Diabetes* 55 (2006) 120–127.

[51] F.F. Martins, T.C.L. Bargut, M.B. Aguila, C.A. Mandarim-de-Lacerda, Thermogenesis, fatty acid synthesis with oxidation, and inflammation in the brown adipose tissue of ob/ob (-/-) mice, *Ann. Anat.* 210 (2017) 44–51, <https://doi.org/10.1016/j.jaanat.2016.11.013>.

[52] P.P. Khedoe, G. Hoeke, S. Kooijman, W. Dijk, J.T. Buijs, S. Kersten, L.M. Havekes, P.S. Hiemstra, J.F. Berbee, M.R. Boon, P.C. Rensen, Brown adipose tissue takes up plasma triglycerides mostly after lipolysis, *J. Lipid Res.* 56 (2015) 51–59, <https://doi.org/10.1199/jlr.M052746>.

[53] M.D. Lynes, L.O. Leiria, M. Lundh, A. Bartelt, F. Shamsi, T.L. Huang, H. Takahashi, M.F. Hirshman, C. Schlein, A. Lee, L.A. Baer, F.J. May, F. Gao, N.R. Narain, E.Y. Chen, M.A. Kiebisch, A.M. Cyphers, M. Bluher, L.J. Goodyear, G.S. Hotamisligil, K.I. Stanford, Y.H. Tseng, The cold-induced lipokine 12,13-diHOME promotes fatty acid transport into brown adipose tissue, *Nat. Med.* 23 (2017) 631–637, <https://doi.org/10.1038/nm.4297>.

[54] S.K. Maloney, A. Fuller, D. Mitchell, C. Gordon, J.M. Overton, Translating animal model research: does it matter that our rodents are cold? *Physiology Bethesda (Bethesda)* 29 (2014) 413–420, <https://doi.org/10.1152/physiol.00029.2014>.

[55] A.V. Kalinovich, J.M. de Jong, B. Cannon, J. Nedergaard, UCPI in adipose tissues: two steps to full browning, *Biochimie* 134 (2017) 127–137, <https://doi.org/10.1016/j.biochi.2017.01.007>.

[56] S.A. Bustin, V. Benes, J.A. Garson, J. Hellemans, J. Huggett, M. Kubista, R. Mueller, T. Nolan, M.W. Pfaffl, G.L. Shipley, J. Vandesompele, C.T. Wittwer, The MIQE guidelines: minimum information for publication of quantitative real-time PCR experiments, *Clin. Chem.* 55 (2009) 611–622, <https://doi.org/10.1373/clinchem.2008.112797>.